# Synthesis and Magnetic Exchange Properties of Linear Trinuclear Oxo-Bridged $M^{III}ORu^{IV}OM^{III}$ Complexes (M = Fe, Cr, Mn) Formed by Two-Electron Redox Reactions

**Kevin J. Berry,[†] Boujemaa Moubaraki,[‡] Keith S. Murray,*[,‡] Peter J. Nichols,[‡] Lewis D. Schulz,[‡] and Bruce O. West*[,‡]**

Westernport Secondary College, Hastings, Victoria, Australia 3915, and Centre of Chemical Synthesis, Department of Chemistry, Monash University, Clayton, Victoria, Australia 3168

*Received December 15, 1994*[⊗]

The two-electron reductions of various porphyrin complexes $Ru^{VI}(O)_2(P)$ by Fe(II), Cr(II), and Mn(II) compounds of porphyrins and salicylaldimines result in the formation of heterotrimetallic oxo-bridged complexes $(L)M^{III}ORu^{IV}(P)OM^{III}(L)$ (M = Fe(III), Cr(III), Mn(III); P is the dianion of 5,10,15,20-tetraarylporphyrins, such as tetraphenylporphyrin (TPP), tetrakis(*p*-methoxyphenyl)porphyrin (TMP), or 2,3,7,8,12,13,17,18-octaethylporphyrin (OEP); L is TPP, TMP, or OEP or the dianions of *N*,*N*′-(4-methyl-4-azaheptane-1,7-diyl)bis(salicylaldimine) (salmah) or *N*,*N*′-ethane-1,2-diylbis(salicylaldimine) (salen). A detailed study of the temperature- and field-dependent magnetic properties of this rather novel series of $(L)M^{III}ORu^{IV}(P)OM^{III}(L)$ compounds has been made. The spin-states of the constituent metal centers are as follows: $Ru^{IV}$, $S_{Ru} = 1$ ($d^4$); $Fe^{III}$, $S_{Fe} = {}^5/_2$ ($d^5$); $Cr^{III}$, $S_{Cr} = {}^3/_2$ ($d^3$); $Mn^{III}$, $S_{Mn} = {}^4/_2$ ($d^4$). The spin-state and coordination geometry of the $(L)Fe^{III}$ groups were confirmed by Mössbauer spectral measurements. Trinuclear combinations of the present kind give rise to unusual coupled spin-state energy levels which, in the case of $(L)Fe^{III}ORu^{IV}(P)OFe^{III}(L)$ compounds, result in "ferromagnetic-like" plots of magnetic moment versus temperature, particularly at low temperatures. The following best-fit values of parameters were deduced from the magnetic moment data, obtained in 1 T fields over the temperature range 4.2–300 K. (salmah)FeORu(TPP)OFe(salmah): $g = 1.97$, $J_{12} = -19.7$ cm$^{-1}$, $J_{13} = +6.5$ cm$^{-1}$, $\alpha = J_{13}/J_{12} = -0.33$, ground-state $S = 4$; (TMP)FeORu(TPP)OFe(TMP): $g = 1.95$, $J_{12} = -23.4$ cm$^{-1}$, $J_{13} = 5.4$ cm$^{-1}$, $\alpha = -0.23$, ground-state $S = 4$. (TPP)FeORu(TPP)OFe(TPP): $g = 2.0$, $J_{12} = -35.7$ cm$^{-1}$, $J_{13} = 11.2$ cm$^{-1}$, $\alpha = -0.31$, ground-state $S = 4$, $[(TPP)Fe]_2O$ impurity = 13%, zero-field splitting of the $S = 4$ state ($D \approx 5$ cm$^{-1}$). (TMP)MnORu(TPP)OMn(TMP): $g = 1.93$, $J_{12} = -17.4$ cm$^{-1}$, $J_{13} = 9.6$ cm$^{-1}$, $\alpha = -0.55$, ground-state $S = 3$. (TPP)CrORu(TPP)OCr(TPP): $g = 1.98$, $J_{12} = -25.3$ cm$^{-1}$, $J_{13} = -11.1$ cm$^{-1}$, $\alpha = 0.44$, ground-state $S = 1$. Possible reasons for the small sizes of the $J_{12}$ values, in comparison to those of related $M^{III}OM^{III}$ and $Ru^{IV}ORu^{IV}$ compounds, are discussed.

## Introduction

While various types of trinuclear bridged d-block complexes have been known for some time,[1] interest in such molecules has been rekindled in recent years because of the identification of trinuclear units or aggregates in iron–sulfur proteins,[2,3] blue copper oxidases,[4] and various phosphatases[5] and nucleases.[6] The majority of known trinuclear oxo-bridged metallic complexes have been prepared by hydrolytic processes involving mixtures of the desired metals in appropriate oxidation states. The well-known triangular homo- and heteronuclear $M_3(\mu_3\text{-O})$ basic carboxylates are synthesized by such processes.[7] The unique series of metal–metal-bonded triangular $M'_2M''$–O-alkoxy compounds (M′ = Mo or W, M″ = W or Mo)[8] were prepared by reaction of $(RO)_3M'{\equiv}M'(OR)_3$ with $M''O(OR)_4$, which may be described as a redox addition process. However, there has not been available a direct method for the specific synthesis of linear heterometallic trinuclear complexes with the oxo group as a ligand.

One-electron redox processes have been successfully used to prepare a range of dinuclear oxo-bridged heterometallic compounds by the reaction of a higher valent metal–oxo compound with a lower valent complex of a different element.[9] Such a reaction was first attempted by Wilson *et al.*,[10] who reacted an Fe(III) porphyrin with a Cu(I) complex attempting to prepare an Fe(III)–O–Cu(II) complex as a possible cytochrome *c* oxidase model. Subsequent examples of this procedure used $Cr^{IV}O$ porphyrins reacting with Fe(II) complexes to yield Cr(III)–O–Fe(III) species,[11,12] the constitutions of which were defined by structural[11,13] Mössbauer spectral and magnetic studies.

$Cr^{III}$–O–$Mn^{III}$,[12] $Cr^{III}$–O–$Mo^{V}$,[12,14] and $Cr^{III}$–O–$V^{V}$ [15] species have also been prepared by related reactions. We have

[†] Westernport Secondary College.
[‡] Monash University.
[⊗] Abstract published in *Advance ACS Abstracts,* July 1, 1995.

(1) Martin, R. L. *New Pathways in Inorganic Chemistry*; Ebsworth, E. A. V., Maddock, A. G., Sharpe, A. G., Eds.; Cambridge University Press: Cambridge, U.K., 1968; Chapter 9.
(2) Fenton, D. E.; Okawa, H. *J. Chem. Soc., Dalton Trans.* **1993**, 1349 and references therein.
(3) Trautwein, A. X.; Bill, E.; Bominaar, E. L.; Winkler, H. *Struct. Bonding* **1991**, *78*, 1 and references therein.
(4) Messerschmidt, A. *Adv. Inorg. Chem.* **1994**, *40*, 121.
(5) Coleman, J. E.; Gettins, P. *Metals in Biology*; Spiro, T. G., Ed.; Wiley: New York, 1983; Vol. 3, Chapter 5.
(6) Lahm, A.; Volbeda, S.; Suck, D. *J. Mol. Biol.* **1990**, *215*, 207.
(7) Cannon, R. D.; White, R. P. *Prog. Inorg. Chem.* **1988**, *36*, 195.
(8) Chisholm, M. H.; Folting, K.; Huffman, J. C.; Kober, E. M. *Inorg. Chem.* **1985**, *24*, 241.
(9) West, B. O. *Polyhedron* **1989**, *8*, 219.
(10) Saxton, R. J.; Olson, L. W.; Wilson, L. J. *J. Chem. Soc., Chem. Commun.* **1982**, 984.
(11) (a) Liston, D. J.; Kennedy, B. J.; Murray, K. S.; West, B. O. *Inorg. Chem.* **1985**, *24*, 1561. (b) Bakshi, E. N.; Elliott, R. L.; Murray, K. S.; Nichols, P. J.; West, B. O. *Aust. J. Chem.* **1990**, *43*, 707.
(12) Elliott, R. L.; Nichols, P. J.; West, B. O. *Aust. J. Chem.* **1986**, *39*, 975.
(13) Fallon, G. D.; Moubaraki, B.; Murray, K. S.; Nichols, P. J.; West, B. O. *Polyhedron* **1993**, *12*.
(14) (a) Elliott, R. L.; Nichols, P. J.; West, B. O. *J. Chem. Soc., Chem. Commun.* **1986**, 840. (b) Elliott, R. L.; Kruger, P.; Murray, K. S.; West, B. O. *Aust. J. Chem.* **1992**, *45*, 889.
(15) Elliott, R. L.; West, B. O. *Aust. J. Chem.* **1988**, *41*, 1417.

0020-1669/95/1334-4123$09.00/0 

now extended this type of reaction to prepare trinuclear species by carrying out two-electron redox reactions on $Ru^{VI}(O)_2$ porphyrins with a variety of metal reductants to give complexes $(L)M^{III}ORu^{IV}(P)OM^{III}(L)$ ($M^{III}$ = Fe, Cr Mn) as shown in eqs 1 and 2.

$$Ru^{VI}(O)_2(P) + M^n(L) \longrightarrow [O{=}Ru^{V}(P){-}O{-}M^{n+1}(L)] \quad (1)$$

$$[O{=}Ru^{V}(P){-}O{-}M^{n+1}(L)] \xrightarrow{M^n(L)} (L)M^{n+1}{-}O{-}Ru^{IV}(P){-}O{-}M^{n+1}(L) \quad (2)$$

A description of the crystal structure of the complex (salmah)-FeORu(TPP)OFe(salmah) has been reported,[16] establishing the bent nature of the Ru−O−Fe bridges in that molecule. The structure is shown again in Figure 1. The structures of two other trimetallic dioxoruthenium species have been previously reported in which the central Ru atom is formally Ru(IV) *viz.* $[(NH_3)_5Ru^{III}{-}O{-}Ru^{IV}(NH_3)_4{-}O{-}Ru^{III}(NH_3)_5]^{6+}$,[17] commonly known as ruthenium red, and $[(NH_3)_5Ru^{III}{-}O{-}Ru^{IV}(en)_2{-}O{-}Ru^{III}(NH_3)_5]^{6+}$,[18] each complex containing a linear Ru−O−Ru−O−Ru spine. The complexes were prepared by hydrolytic reactions.

In the previous report[16] some brief mention was made of the unusual magnetic properties being observed for the FeORuOFe complexes. This paper reports details of the synthesis of these novel complexes together with detailed magnetic studies of a number of them. Particular interest is provided by the inclusion of a second-row d-block ion, Ru(IV) (with spin $S_{Ru} = 1$), at the center of the structure. There are only a few other mixed-metal ruthenium compounds known of the spin-coupled type, and these contain dinuclear combinations such as $Cu^{II}{-}Ru^{III}$, $V^{III}{-}Ru^{III}$, $Mn^{III}{-}Ru^{III}$, $Fe^{III}{-}Ru^{III}$ and $Fe^{III}{-}Ru^{IV}$, the first of which shows ferromagnetic coupling, the others antiferromagnetic.[19-21] The magnetic properties of spin-coupled Ru compounds are not, in general, as well understood as are those of the 1st-row d-block congeners.

A number of significant findings have emerged in the last few years in regard to linear trinuclear compounds, and the unique magnetic exchange properties of such molecules has become of great interest pointing to their potential use in the design of new molecular magnetic materials.[22,23] Thus, the exchange interaction between the terminal metals can generally not be ignored and it is usually as important as the nearest neighbor interaction. This long distance coupling can occur via some rather unexpected central pathways.[24-31] We show, below, that the ratio $J_{13}/J_{12} = \alpha$ is actually the important

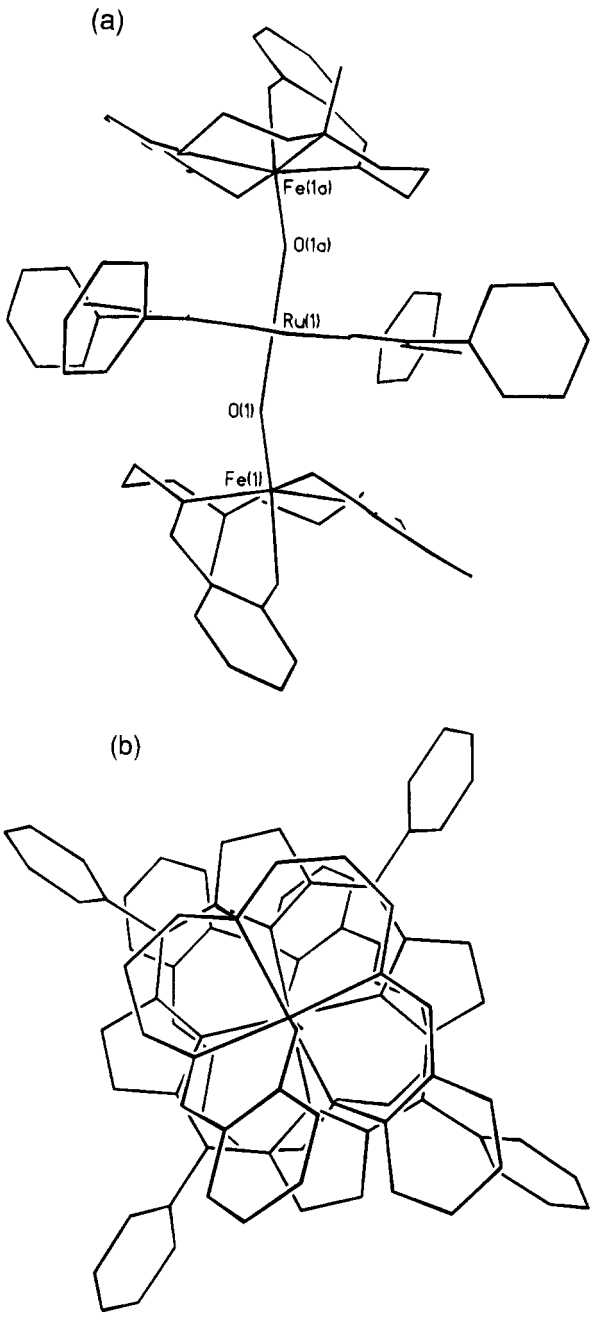


**Figure 1.** (a) Stick diagram of the structure of (salmah)FeORu(TPP)-OFe(salmah). (For crystallographic details, see ref 16). Pertinent distances (Å) and angles (deg) include the following: Fe(1)−O(1) = 1.848(6), Ru(1)−O(1) = 1.866(6), Fe(1)···Ru(1) = 3.63, Fe(1)···Fe-(1a) = 7.25; Fe(1)−O(1)−Ru(1) = 155.2(5), O(1)−Fe(1)−O(phenolate) = 175.2(3). (b) View down the Fe···Ru···Fe spine. The metal−donor atom bonds are eclipsed with respect to each other.

determinant of the ground-state energy level.[1,22] Experimentally, it is most important to measure magnetization isotherms at very low temperatures in order to determine the ground-state and the low-lying energy levels. Further, the thermodynamic form of magnetization (and susceptibility), which contains a magnetic field term, must be used, in combination with matrix-diagonalization of the appropriate Hamiltonian, to correctly reproduce the magnetic data. Also in the case of mixed-metal and hence in mixed-spin systems, some rather unusual and irregular spin-

(16) Schulz, L. D.; Fallon, G. D.; Moubaraki, B.; Murray, K. S.; West, B. O. *J. Chem. Soc., Chem. Commun.* **1992**, 971.
(17) Fletcher, J. M.; Garder, W. E.; Hooper, E. W.; Hyder, K. R.; Moore, F. H.; Woodhead, J. L. *Nature (London)* **1963**, *199*, 1089.
(18) Smith, P. M.; Fealey, T.; Earley, J. E.; Silverton, J. V. *Inorg. Chem.* **1971**, *10*, 1943.
(19) Inoue, K.; Matsumoto, N.; Okawa, H. *Chem. Lett.* **1993**, 1433.
(20) Hotzelmann, R.; Wieghardt, K.; Flörke, U.; Haupt, H.-J. *Angew. Chem., Int. Ed. Engl.* **1990**, *29*, 643.
(21) Hotzelmann, R.; Wieghardt, K.; Ensling, J.; Romstedt, H.; Gütlich, P.; Bill, E.; Flörke, U.; Haupt, H.-J. *J. Am. Chem. Soc.* **1992**, *114*, 9470.
(22) Kahn, O. *Molecular Magnetism*; VCH: New York, 1993.
(23) Pei, Y.; Journaux, Y.; Kahn, O. *Inorg. Chem.* **1988**, *27*, 399.
(24) Chaudhuri, P.; Winter, M.; Fleischauer, P.; Haase, W.; Flörke, U.; Haupt, H.-J. *Inorg. Chem.* **1991**, *30*, 4777.
(25) Chaudhuri, P.; Winter, M.; Fleischauer, P.; Haase, W.; Flörke, U.; Haupt, H.-J. *J. Chem. Soc., Chem. Commun.* **1990**, 1728.
(26) Pei, Y.; Journaux, Y.; Dei, A.; Gatteschi, D. *J. Chem. Soc., Chem. Commun.* **1986**, 1300.
(27) Zhang, J. H.; Flomer, W. A.; Kolis, J. W.; O'Connor, C. J. *Inorg. Chem.* **1990**, *29*, 1108.
(28) Borer, L. L.; Horsma, R.; Rajan, O. A.; Sinn, E. *Inorg. Chem.* **1986**, *25*, 3652.
(29) Rardin, R. L.; Poganiuch, P.; Bino, A.; Goldberg, D. P.; Tolman, W. B.; Liu, S.; Lippard, S. J. *J. Am. Chem. Soc.* **1992**, *114*, 5240.
(30) Ginsberg, A. P.; Martin, R. L.; Sherwood, R. C. *Inorg. Chem.* **1968**, *7*, 932.
(31) Haase, W.; Gehring, S. *J. Chem. Soc., Dalton Trans.* **1985**, 2609.

state ladders are possible with some consequently unusual $\mu$ (or $\chi$) versus temperature plots, including those having a minimum on account of the coupled ground state having a higher spin than some of the upper levels.[23-26] This behavior is reminiscent of the behavior of ferrimagnetic chains,[22] and a number of groups are attempting to develop molecular designs which hopefully will prove useful in obtaining very high-spin ground-state molecular fragments, leading ultimately to spontaneous 3-dimensional magnetic ordering.

## Experimental Section

**Materials and Techniques.** All chemical operations were carried out under nitrogen (pretreated by passage through BASF R311 catalyst to remove traces of oxygen and BDH 4A molecular sieves to remove water) using standard Schlenk techniques. Solvents were dried by standard methods. Tetrahydrofuran and toluene were distilled from benzophenone ketyl under nitrogen immediately before use. Triruthenium dodecacarbonyl was supplied by Aldrich or synthesized directly from ruthenium trichloride. Spectra were recorded as follows: UV/visible, Hitachi 150-20; infrared, PE FT 1600; $^1$H NMR, Bruker AM 300. Electron microprobe analyses were used extensively to check the metal ratios in reaction products as a measure of their purity and homogeneity. A Jeol JSM 840A scanning electron microscope was used, linked through an NEC X-ray detector and pulse processing system to a Link System 860 analyzer. Samples were mounted on aluminium planchettes and coated with carbon using a Balzer Union CED-010 carbon sputterer. The finely focused electron beam was able to give metal analyses (±10%) of selected areas in a sample of the order of $10^{-2}$ mm$^2$. This accuracy was an invaluable preliminary check on the purity of preparations of the trinuclear species. Mixtures of solid Ru(O)$_2$(TPP) and Fe(TPP)(pip)$_2$ or appropriate Cr and Mn complexes in 1:2 ratios were ground together to act as standards initially. Once the complex (salmah)FeORu(TPP)OFe(salmah) had been crystallographically characterized, samples of that compound were used as a standard.

Microanalyses were performed by the National Analytical Laboratories, Melbourne, Australia.

**Magnetic Susceptibility and Mössbauer Spectral Measurements.** Room-temperature magnetic moments were measured on a Faraday balance, designed and built in the Monash Chemistry Department, which incorporated a Cahn balance and a Newport 4 in. electromagnet, the latter fitted with Faraday profile pole-pieces. The absence of field-dependent impurities was regularly checked by varying the magnetic field over the range 0.05−1 T. The variable-temperature data were obtained using a Quantum Design MPMS Squid magnetometer. Powdered samples of mass *ca.* 20 mg were contained in calibrated gelatine capsules which were inserted into the middle of a soda straw attached to the end of the sample rod. The instrument was regularly calibrated against a standard metallic palladium sample and chemical calibrants such as CuSO$_4$·5H$_2$O, [Ni(en)$_3$]S$_2$O$_3$, and Hg[Co(NCS)$_4$]. In the case of the variable-field measurements (0.1−5.0 T), made at low temperatures, care was taken to check that no torquing caused by crystallite orientation was occurring (see ref 56) thus leading to anomalous values of magnetic moment. This was done by (i) carefully raising and then lowering the field at a fixed temperature and noting that the magnetization values exactly reproduced themselves and (ii) making measurements on loose powdered samples and then on compressed powdered samples and noting that the magnetization values were very similar over the whole temperature range.

Mössbauer spectral measurements were made using instruments constructed in the Physics Department, Monash University.[11] Isomer shifts are calibrated relative to α-iron.

**Porphyrins.** (TPP)H$_2$ and (TMP)H$_2$ were prepared by the general literature method,[32] chlorin impurities being removed by treatment with 2,3-dichloro-5,6-dicyanobenzoquinone (DDQ).[33] (OEP)H$_2$ was synthesized by the method of Sessler.[34] Each porphyrin was finally purified by chromatography in CH$_2$Cl$_2$ solution on basic alumina (activity 2).

**Ruthenium Porphyrin Complexes.** Ru(TPP)(CO)(EtOH), Ru(TMP)(CO)(EtOH), and Ru(OEP)(CO)(MeOH) were prepared by literature methods replacing RuCl$_3$·H$_2$O[35] with Ru$_3$(CO)$_{12}$.[36]

**Dioxoruthenium(VI) Porphyrin Complexes.** Ru$^{VI}$(O)$_2$(TPP), Ru$^{VI}$(O)$_2$(OEP), and Ru$^{VI}$(O)$_2$(TMP) were prepared by the method of Che *et al.*[37,38]

**Dioxo(5,10,15,20-tetraphenylporphyrinato)ruthenium(VI) [Ru(O)$_2$(TPP)].** Ru(TPP)CO(EtOH) (0.4 g) was dissolved in a CH$_2$Cl$_2$/EtOH mixture (9:1, 40 mL), and the solution was filtered and added to a solution of *m*-chloroperbenzoic acid (6 g) in EtOH (400 mL). After 1 h the precipitated product was filtered out and washed several times with EtOH. Yield: 75%. Anal. Calcd for C$_{44}$H$_{28}$N$_4$O$_2$Ru: C, 71.0; H, 4.1; N, 7.4. Found: C, 71.0; H, 3.8; N, 7.5. UV/vis (CH$_2$Cl$_2$) ($\lambda_{max}$, nm): 419, 520, 550 sh (lit.[37] 418, 518, 550 sh).

**Dioxo(5,10,15,20-tetrakis(*p*-methoxyphenyl)porphyrinato)ruthenium(VI) [Ru(O)$_2$(TMP)].** Anal. Calcd for C$_{48}$H$_{36}$N$_4$O$_6$Ru: C, 66.6; H, 4.2; N, 6.5. Found: C, 66.5; H, 4.3; N, 6.3. UV/vis (CH$_2$Cl$_2$) ($\lambda_{max}$, nm): 420, 524, 560.

**Dioxo(2,3,7,8,12,13,17,18-octaethylporphyrinato)ruthenium(VI) [Ru(O)$_2$(OEP)].** Anal. Calcd for C$_{36}$H$_{44}$N$_4$O$_2$Ru: C, 64.7; H, 6.7; N, 8.5. Found: C, 64.7; H, 6.7; N, 8.4. UV/vis (CH$_2$Cl$_2$) ($\lambda_{max}$, nm): 393, 508, 542 (lit.[37] 396, 508, 540).

**Fe(II), Cr(II), and Mn(II) Porphyrins.** Fe(TPP)(pip)$_2$ and Fe(TMP)(pip)$_2$ were prepared by the reaction of Fe$^{III}$(P)Cl compounds with piperidine in CH$_2$Cl$_2$ under argon.[39] Cr$^{III}$(TPP)Cl[40,41] was reduced by chromium(II) acetylacetonate (Cr$_2$(acac)$_4$)[42] in a toluene/ethanol mixture (50:1) to yield Cr$^{II}$(TPP) as the di-toluene solvate.[43] The Mn$^{II}$(P) compounds were prepared by reduction of Mn$^{III}$(TPP)Cl or Mn$^{III}$(TMP)Cl[44] with NaBH$_4$ in methanol/pyridine (1:1) solution and isolated by addition of further methanol as the monopyridinates.

Fe$^{II}$(salmah) and Fe$^{II}$(salen)(py) were prepared by the reaction of Fe(py)$_4$(NCS)$_2$ with the appropriate salicylaldimine in ethanol in the presence of triethylamine.[12] The Schiff bases were prepared *in situ* by reacting salicylaldehyde and diamine in ethanol.

**Synthesis of (L)M$^{III}$ORu$^{IV}$(P)OM$^{III}$(L) (M = Fe, Cr, Mn) Heterotrinuclear Oxo-Bridged Complexes.** The following description is typical of the procedures followed to prepare the oxo-bridged compounds. Toluene was used as the solvent for reactions involving Fe salicylaldimines, but CH$_2$Cl$_2$ was the solvent in all other reactions because of its greater solvent properties for the various metal porphyrins. The isolated complexes were in general poorly soluble in most common solvents. At the low concentrations required for measurement of the UV/visible spectra of most of the complexes (*ca.* $10^{-6}$ M) the spectra showed changes with time or had initial absorption bands indicating that decomposition had occurred giving M$^{III}$ and probably [Ru$^{IV}$(P)OH]$_2$O species due to attack by traces of moisture despite the precautions taken. Accordingly only those spectra considered to represent the undecomposed complexes are recorded. Decomposition was particularly obvious among the Cr(III) and Mn(III) complexes, and no spectra are reported for these compounds. Microanalytical data

(32) Adler, A. D.; Longo, F. R.; Finarelli, J. D.; Goldmacher, J.; Assour, J.; Korskakoff, L. *J. Org. Chem.* **1967**, *32*, 476.
(33) Barnett, G. H.; Hudson, M. F.; Smith, K. M. *J. Chem. Soc., Perkin Trans. 1* **1975**, 1401.
(34) Sessler, J. L.; Mozaffari, A.; Johnson, M. R. *Organic Syntheses*; Wiley: New York, 1992; Vol. 70, p 68.
(35) Collman, J. P; Barnes, C. E.; Brothers, P. J.; Collins, T. J.; Ozawa, T.; Gallucci, J. C.; Ibers, J. A. *J. Am. Chem. Soc.* **1984**, *106*, 5151.
(36) Antipas, A.; Buchler, J. W.; Gouterman, M.; Smith, P. D. *J. Am. Chem. Soc.* **1978**, *100*, 3015.
(37) Leung, W.-H.; Che, C.-M. *J. Am. Chem. Soc.* **1989**, *111*, 8812.
(38) Ho, C.; Leung, W.-H.; Che, C.-M. *J. Chem. Soc., Dalton Trans.* **1991**, 2933. Che, C.-M.; Yam, V. W.-W. *Adv. Inorg. Chem.* **1992**, *39*, 233.
(39) Epstein, L. M.; Straub, D. K.; Maricondi, C. *Inorg. Chem.* **1967**, *6*, 1720.
(40) Adler, A. D.; Longo, F. R.; Kampas, K.; Kim, J. *J. Inorg. Nucl. Chem.* **1970**, *32*, 2443.
(41) Jones, R. D.; Summerville, D. A.; Hoffman, B. M.; Basolo, F. *J. Am. Chem. Soc.* **1978**, *100*, 4416.
(42) Ocone, L. R.; Block, B. P. *Inorg. Synth.* **1966**, *8*, 125.
(43) Cheung, S. K.; Grimes, C. J.; Wong, J.; Reed, C. A. *J. Am. Chem. Soc.* **1976**, *98*, 5928.
(44) Jones, R. D.; Summerville, D. A.; Basolo, F. *J. Am. Chem. Soc.* **1978**, *100*, 4416. Hoffman, B. M.; Szymanski, T.; Brown, T. G.; Basolo, F. *J. Am. Chem. Soc.* **1978**, *100*, 7253.

and specific infrared measurements have been collected in supporting information Table S1.

**Bis{(μ-oxo)[*N,N'*-(4-methyl-4-azaheptane-1,7-diyl)bis(salicylaldiminato)iron(III)]}−[(5,10,15,20-Tetraphenylporphyrinato)ruthenium(IV)] [(salmah)FeORu(TPP)OFe(salmah)].** A suspension of $Ru(O)_2$(TPP) (160 mg, 0.215 mmol) in dry, deoxygenated toluene (20 mL) was added to a red solution of $Fe^{II}$(salmah) (175 mg, 0.430 mmol) also in toluene (10 mL). The brown solution so formed developed an olive green color over a period of 10 min. After being stirred at room temperature for a further 1.5 h, the solution was filtered, dry hexane added, and the mixture cooled in ice. The purple microcrystalline product was collected and washed with hexane. The compound was not solvated with toluene. Yield: 110 mg, 30%. $\mu_{eff}$ (295 K) = 8.25 $\mu_B$. UV/vis (toluene) [$\lambda_{max}$, nm (log $\epsilon$)]: 350 (4.59) sh, 425 (5.02) (Soret), 500 (4.36), 602 (4.25). This spectrum was unchanged for 5 min. However after 24 h it had changed to a Soret type band at 410 nm with a less intense peak at 520 nm. The crystals used for the X-ray diffraction study[16] were recrystallized from $CH_2Cl_2$ and contained 4 mol of $CH_2Cl_2$ per trimer unit. The Ru(TMP) and (OEP) complexes were prepared similarly.

**Bis{(μ-oxo){*N,N'*-(4-methyl-4-azaheptane-1,7-diyl)bis(salicylaldiminato)iron(III)}−[(5,10,15, 20-Tetrakis(*p*-methoxyphenyl)porphyrinato)ruthenium(IV)] [(salmah)FeORu(TMP)OFe(salmah)].** Yield: 15%. UV/vis ($CH_2Cl_2$) ($\lambda_{max}$, nm): 416 (Soret), 531, 570, 600. $\mu_{eff}$ (295 K) = 7.35 $\mu_B$.

**Bis{(μ-oxo)[*N,N'*-(4-methyl-4-azaheptane-1,7-diyl)bis(salicylaldiminato)iron(III)]}−[(2,3,7,8,12,13,17,18-Octaethylporphyrinato)ruthenium(IV)] [(salmah)FeORu(OEP)OFe(salmah)].** Yield: 10%. UV/vis ($CH_2Cl_2$) ($\lambda_{max}$, nm): 390 (Soret) 450, 500, 550, 600. $\mu_{eff}$ (295 K) = 8.6 $\mu_B$.

**Bis{(μ-oxo)[5,10,15,20-tetraphenylporphyrinato)iron(III)]}−[5,10,15,20-Tetraphenylporphyrinato)ruthenium(IV)] [(TPP)FeORu(TPP)OFe(TPP)].** $Ru(O)_2$(TPP) (100 mg, 0.134 mmol) and Fe(TPP)(pip)$_2$ (225 mg, 0.268 mmol) were dissolved in $CH_2Cl_2$ (30 mL), and the solution was stirred. A dark red purple microcrystalline product precipitated after approximately 10 min and was collected and washed with hexane. Yield: 30%. UV/vis (tol/$CH_2Cl_2$, 1:5) [$\lambda_{max}$, nm (log $\epsilon$)]: 403 (5.22) (Soret), 523, 575, 613 (unchanged for 5 min). $\mu_{eff}$ (295 K) = 8.1 $\mu_B$.

Similar procedures were used to prepare the other Fe(P), Cr(P), and Mn(P) complexes. The precursor complexes Cr(TPP)·2tol and Mn(P)py were employed.

**Bis{(μ-oxo)[(5,10,15,20-tetrakis(*p*-methoxyphenyl)porphyrinato)iron(III)]}−[(5,10,15,20-Tetraphenylporphyrinato)ruthenium(IV)] [(TMP)FeORu(TPP)OFe(TMP)].** Yield: 10%. UV/vis ($CH_2Cl_2$) ($\lambda_{max}$, nm): 408 (Soret), 518, 572, 615. $\mu_{eff}$ (295 K) = 8.2 $\mu_B$.

**Bis{(μ-oxo)[(5,10,15,20-tetrakis(*p*-methoxyphenyl)porphyrinato)iron(III)]}−[(5,10,15,20-Tetrakis(*p*-methoxyphenyl)porphyrinato)ruthenium(IV)] [(TMP)FeORu(TMP)OFe(TMP)].** Yield: 15%. UV/vis ($CH_2Cl_2$) ($\lambda_{max}$, nm): 408 (Soret), 522, 576, 618. $\mu_{eff}$ (295 K) = 7.9 $\mu_B$.

**Bis{(μ-oxo)[(5,10,15,20-tetraphenylporphyrinato)chromium(III)]}−[(5,10,15,20-tetraphenylporphyrinato)ruthenium(IV)] [(TPP)CrORu(TPP)OCr(TPP)].** Yield: 50%. $\mu_{eff}$ (295 K) = 5.2 $\mu_B$.

**Bis{(μ-oxo)[(5,10,15,20-tetraphenylporphyrinato)chromium(III)}−[(5,10,15,20-Tetrakis(*p*-methoxyphenyl)porphyrinato)ruthenium(IV)] [(TPP)CrORu(TMP)OCr(TPP)].** Hexane was required to precipitate the compound in this preparation. Yield: 15%. $\mu_{eff}$ (295 K) = 5.8 $\mu_B$.

**Bis{(μ-oxo)[(5,10,15,20-tetraphenylporphyrinato)manganese(III)]}−[(5,10,15,20-Tetraphenylporphyrinato)ruthenium(IV)] [(TPP)MnORu(TPP)OMn(TPP)].** Yield: 32%. $\mu_{eff}$ (295 K) = 7.0 $\mu_B$.

**Bis{(μ-oxo)[(5,10,15,20-tetrakis(*p*-methoxyphenyl)porphyrinato)manganese(III)]}−[(5,10,15,20-Tetraphenylporphyrinato)ruthenium(IV)] [(TMP)MnORu(TPP)OMn(TMP)].** Yield: 20%. $\mu_{eff}$ (295 K) = 7.0 $\mu_B$.

**Bis{(μ-oxo)[(5,10,15,20-tetrakis(*p*-methoxyphenyl)porphyrinato)manganese(III)]}−[(5,10,15,20-Tetraphenylporphyrinato)ruthenium(IV)] [(TMP)MnORu(TMP)OMn(TMP)].** Yield: 20%. $\mu_{eff}$ (295 K) = 5.5 $\mu_B$.

**Bis{(μ-oxo)[(5,10,15,20-tetraphenylporphyrinato)manganese(III)]}−[(2,3,7,8,12,13,17,18-Octaethylporphyrinato)ruthenium(IV)] [(TPP)MnORu(OEP)OMn(TPP)].** Yield: 15%. $\mu_{eff}$ (295 K) = 7.2 $\mu_B$.

**Reactions Which Did Not Yield Heterotrinuclear Species. Ru(O)$_2$(TPP) and Fe(salen)(py).** A suspension of $Ru(O)_2$(TPP) (70 mg, 0.09 mmol) in toluene (15 mL) was added to a suspension of Fe(salen)(py) (75 mg, 0.18 mmol) in toluene, and an orange solution with a dark orange precipitate rapidly resulted. After 1 h the solution was filtered and the dark orange solid filtered off and identified as [Fe(salen)]$_2$O by comparison of its IR spectrum with that of an authentic sample. The filtrate was cooled to 0 °C, pentane was added, and a purple solid precipitated. It was identified as $Ru^{II}$(TPP)(py)$_2$ by its absorption spectrum.[45] $Ru(O)_2$(OEP) and Fe(salen)(py) reacted similarly. The reaction of $Ru(O)_2$(TPP) and Fe(salen) in dry tetrahydrofuran also yielded [Fe(salen)]$_2$O and Ru(TPP)(thf)$_2$.[35]

**Ru(O)$_2$(OEP) and Fe(TPP)(pip)$_2$.** $CH_2Cl_2$ (20 mL) was added to a mixture of the solids $Ru(O)_2$(OEP) (40 mg, 0.06 mmol) and Fe(TPP)(pip)$_2$ (100 mg, 0.12) resulting in the formation of a red-brown solution. After 1 h the solution was filtered, reduced to about half-volume by flow of nitrogen, and cooled to 0 °C. [Fe(TPP)]$_2$O was precipitated (identified by comparison of its IR spectrum with an authentic sample). The red-colored filtrate had a visible spectrum indicative of a disolvated $Ru^{II}$(OEP)(B)$_2$ complex[36] (UV/vis for $Ru^{II}$(OEP)(pip)$_2$ ($\lambda_{max}$, nm): 393 (Soret), 494, 520).

## Results and Discussion

**Synthesis and Characterization of (L)MORu(P)OM(L) Complexes.** $Ru^{VI}(O)_2$ porphyrin compounds have been found to react rapidly with $Fe^{II}$(salmah) and Fe(II), Cr(II), and Mn(II) porphyrins in toluene or $CH_2Cl_2$ solution. Fe(salmah) is reasonably soluble in either solvent, but the Ru dioxo compounds and the other metalloporphyrins have only modest solubilities. However when the reactants are brought together, the mixture tends to dissolve fairly readily and a product precipitates from solution in a matter of minutes in a number of instances. In other cases hexane must be added to obtain a product. The yields of solid complexes obtained are not high, ranging from as low as 10% for (TMP)FeORu(TPP)OFe(TMP) to 50% in the case of the (TPP)CrORu(TPP)OCr(TPP). Attempts to increase the yields of compounds by addition of large amounts of precipitating solvents or reduction of solution volumes were generally unsuccessful. The X-ray structural study of (salmah)FeORu(TPP)OFe(salmah) performed on a $4CH_2Cl_2$ solvate[16] confirmed the oxo-bridged trinuclear nature of that complex (Figure 1). Although no other crystal suitable for an X-ray study was obtained of any of the many other complexes prepared, the properties of the remaining compounds, particularly their reduced magnetic moments, indicate similar trinuclear constitutions.

In reactions of the various $Fe^{II}$(P)(pip)$_2$ species with $Ru^{VI}(O)_2$(P) compounds, although small yields of the expected trinuclear complexes were precipitated rapidly on mixing the reagents, examination of the filtrates of the mixtures showed the presence of the relevant $[Fe^{III}(P)]_2O$ compounds. Other examples of particular reaction mixtures described in the Experimental Section gave no isolable quantities of trinuclear species, but $[Fe^{III}]_2O$ and $Ru^{II}$(P) species were obtained. These observations are consistent with a reaction sequence in which an initial formation of trinuclear species occurs as in eq 3

$$2Fe^{II}(L) + Ru^{VI}(O)_2(P) \rightleftharpoons \{(L)Fe^{III}-O-Ru^{IV}(P)-O-Fe^{III}(L)\} \quad (3)$$

followed by dissociation of the trinuclear species to the initial

(45) Collman, J. P.; Barnes, C. E.; Swepston, P. N.; Ibers, J. A. *J. Am. Chem. Soc.* **1984**, *106*, 3500.

reactants or new reactive species as in (4). Irreversible

$$(L)Fe^{III}-O-Ru^{IV}(P)-O-Fe^{III}(L) \rightleftharpoons 2Fe^{IV}O(L) + Ru^{II}(P) \quad (4)$$

comproportionation can then form $[Fe^{III}(L)]_2O$ complexes

$$Fe^{IV}O(L) + Fe^{II}(L) \rightarrow [Fe^{III}(L)]_2O \quad (5)$$

The extent of reaction 4 for a given combination of reactants will influence the yield of trinuclear compound. The ability[45] of $Ru^{II}(P)$ to form dimers $[Ru^{II}(P)]_2$ or to be stabilized by formation of $Ru^{II}(P)(L)_2$, where L is pyridine or a similar base initially coordinated to the Fe(II) reagent, will obviously also play a part in determining the position of equilibrium of reaction 4. $Fe^{II}$(salmah) was found to give the highest yields of all Fe(II) complexes studied, and it is no doubt significant that crystalline $[Fe^{III}(salmah)]_2O$ has not previously been reported, the reaction between $Fe^{II}$(salmah) and oxygen (where $Fe^{IV}O$(L) species are expected) being rather slow in chloroform solution.[46]

Homobinuclear oxo-bridged compounds of Mn(III) or Cr(III) have not been isolated as major products of any of the reactions involving $Ru^{VI}(O)_2(P)$ and the $Mn^{II}(P)$ or $Cr^{II}(P)$ compounds used in this work. Although the same set of equilibria (3)−(5) can be envisaged for these metals as for the Fe systems, a combination of greater solubility and/or greater degree of reversibility in the comproportionation reactions of type (5) (as has been demonstrated for the $Cr^{III}_2O$ porphyrin species[47] ) appears to have facilitated the isolation of the trinuclear complexes. Although still relatively uncommon,[48] other examples of such oxo group transfer between dissimilar metals have been recognized.[49]

The UV/visible spectra of freshly dissolved samples of all the trinuclear compounds are given in the Experimental Section. All the spectra showed changes over time in line with dissociation of the compounds. Indeed the $Cr^{III}ORu^{IV}OCr^{III}$ and analogous Mn(III) complexes showed evidence for separate Cr(III) and Mn(III) species immediately on dissolution.[41,44] The Ru porphyrin components in these very dilute solutions showed, after some hours, the characteristic spectra of $[Ru^{IV}]_2O$ species presumably from reaction of Ru(II) with traces of air or moisture.[35]

Some independent evidence of the oxidation state of the Ru in solid samples of these trinuclear compounds is given by the appearance of infrared spectral bands at or near 1012 cm$^{-1}$ (Table S1) which are indicative of Ru(IV) porphyrin compounds.[37,50,51] The FeORuOFe compounds with porphyrin ligands attached to each metal also showed a broad, intense band or shoulder in the region 810−825 cm$^{-1}$ in their infrared spectra, a feature not shown by the Fe(salmah) complexes. These absorptions are tentatively assigned to vibrations arising in their FeORuOFe bond systems. The infrared spectra of dinuclear FeOCr porphyrin compounds showed bands in the vicinity of 860 cm$^{-1}$ assigned to the FeOCr stretching frequency.[11a]

Structural and magnetic studies (*vide infra*) show that solid samples of the trinuclear complexes are discrete phases and not mixtures of the species obtained on aging of their dilute solutions.

**Magnetic and Mössbauer Spectral Properties.** The spin state of $Fe^{III}$ in the complex (salmah)FeORu(TPP)OFe(salmah) was confirmed as $^5/_2$ from Mössbauer spectral measurements. An asymmetric quadrupole doublet was observed at 295 K, with $\delta = 0.43$ mm s$^{-1}$, $\Delta E_Q = 1.31$ mm s$^{-1}$, $I_1/I_2 = 0.63$, and at 77 K, with $\delta = 0.56$ mm s$^{-1}$, $\Delta E_Q = 1.24$ mm s$^{-1}$, and $I_1/I_2 = 0.44$. Such data are typical of six-coordinate $Fe^{III}$ Schiff base centers.[52] The Mössbauer parameters for (TPP)FeORu(TPP)OFe(TPP) are also indicative of high-spin Fe(III), the size of $\Delta E_Q$ being indicative of five-coordinate geometry: $\delta = 0.35$ mm s$^{-1}$, $\Delta E_Q = 0.62$ mm s$^{-1}$, $I_1/I_2 = 0.52$ (295 K); $\delta = 0.43$ mm s$^{-1}$, $\Delta E_Q = 0.65$ mm s$^{-1}$, $I_1/I_2 = 0.38$ (77 K).[53] The spin state of $S_{Ru} = 1$ on the $Ru^{IV}$ porphyrin moiety was evident from the analysis of the magnetic data. We have previously shown how the Ru−O distances in various $Ru^{IV}$ compounds, including $\mu$-oxo−porphyrin species, supports this assignment.[16] Notable in this regard, is the structure of a triply-bridged heterobinuclear Ru−$\mu$-oxo complex recently published by Wieghardt *et al.*,[21] in which Ru is proposed to have the IV oxidation state, *viz.* $[(tacn)Fe^{III}(\mu\text{-}O)(\mu\text{-}CH_3CO_2)_2Ru^{IV}(Me\text{-}tacn)](PF_6)_3$. In this case, Fe−O = 1.86 Å, Ru−O = 1.82 Å, and Fe−O−Ru = 121°. The Ru−O distance is shorter than in the trinuclear complex, and the bridge angle is, of course, smaller. A spin of 1 was assigned to $Ru^{IV}$ and a resonance structure Ru=O−Fe suggested to contribute to the bonding in the bridge.[21] An alternative possibility that the $S_{Ru} = 1$ state in the present trimer derives from a low-spin $Ru^{III}$−porphyrin cation radical $TPP^{+\bullet}$ can be eliminated since the UV/vis and IR spectra give no evidence for the $\pi$-cation radical species.[54] As indicated earlier, the IR band at 1012 cm$^{-1}$ in this and the other Ru(P) complexes is indicative of $Ru^{IV}$(P). The spin state on $Mn^{III}$ in the analogous trinuclear complex is $S_{Mn} = 2$ by analogy to the situation in many polynuclear $Mn^{III}$ Schiff base complexes. $Cr^{III}$ is unambiguously $S_{Cr} = {}^3/_2$.

The detailed magnetic data, and their analyses, are now given individually for representative complexes. Six examples of FeRuFe complexes were made with all, except one, having $\mu$ values of *ca.* 8.2 $\mu_B$ at 295 K. The lower value obtained for the RuTMP species (7.3−7.9 $\mu_B$), noted also in the MnRuMn group, may reflect chemical instability rather than a different degree of coupling.

**(a) (salmah)FeORu(TPP)OFe(salmah).** The plot of $\mu$ (per mol) versus temperature, in an applied field of 1 T, is shown in Figure 2a. The $\mu$ value at room temperature of 8.25 $\mu_B$ increases gradually toward a maximum value of 8.8 $\mu_B$ at *ca.* 20 K before decreasing rapidly, reaching a value of 7.95 $\mu_B$ at 4.2 K. Such behavior is "ferromagnetic-like" in nature, the $\mu_{max}$ value being close to that expected for a spin = 4 state ($\mu_{calc} = 8.94$ $\mu_B$) arising from the parallel coupling of spins ($^5/_2 + {}^5/_2$) on the $Fe^{III}$ atoms being antiparallel to that ($S_2 = {}^2/_2$) on the $Ru^{IV}$ center.

Confirmation of the $|S,S^*> = |4,5>$ ground state is provided by magnetization data, obtained using fields of 0.1, 0.3, 1.0, and 3.0 T over the temperature range 4.2−300 K. The $\mu$/temperature behavior is independent of field in the range 70−300 K but is very sensitive to variation in applied field in the range 4.2−70 K. The value of $\mu_{max}$ changes from 9.2 $\mu_B$ at 0.1 T to 8.7 $\mu_B$ at 3 T, and the corresponding temperature at the maxima increases from *ca.* 10 K to *ca.* 29 K. The value of $\mu$

(46) Niswander, R. H.; Martell, A. E. *Inorg. Chem.* **1978**, *17*, 1511.
(47) Liston, D. J.; West, B. O. *Inorg. Chem.* **1985**, *24*, 1568.
(48) Holm, R. H. *Chem. Rev.* **1987**, *87*, 1401.
(49) Dailey, G. C.; Horwitz, C. P. *Inorg. Chem.* **1992**, *31*, 3693.
(50) Groves, J. T.; Ahn, K.-H. *Inorg. Chem.* **1987**, *26*, 3831.
(51) Huang, J.-S.; Che, C.-M.; Li, Z.-Y.; Poon, C.-K. *Inorg. Chem.* **1992**, *31*, 1313.
(52) Kennedy, B. J.; Brain, G.; Horn, E.; Murray, K. S.; Snow, M. R. *Inorg. Chem.* **1985**, *24*, 1647.
(53) Sams, J. R.; Tsin, T. B. In *The Porphyrins*; Dolphin, D., Ed.; Academic: New York, 1978; Vol. IV, Chapter 9.
(54) (a) Gans, P.; Buisson, G.; Duee, E.; Marchon, J.-C.; Erler, B. S.; Scholz, W. F.; Reed, C. A. *J. Am. Chem. Soc.* **1986**, *108*, 1223. (b) Czernuszewicz, R. S.; Macor, K. A.; Li, X.-Y.; Kincaid, J. R.; Spiro, T. G. *J. Am. Chem. Soc.* **1989**, *111*, 3860.

at 4.2 K correspondingly decreases from 9.0 $\mu_B$ to 6.05 $\mu_B$ as $H$ changes from 0.1 to 3.0 T. The rapid decrease with temperature of $\mu$ below $\mu_{max}$, particularly at higher applied-field values, appeared at first to be possibly due to zero-field splitting of the ground state or to intertrinuclear antiferromagnetic coupling effects. Theoretical treatment, using the usual Heisenberg spin Hamiltonian (eq 6) for a linear ABA trimer in

$$\begin{matrix} A-B-A \\ S_1 \quad S_2 \quad S_3 \end{matrix}$$

$$\mathcal{H}_{exch} = -2J_{12}(\mathbf{S}_1\cdot\mathbf{S}_2 + \mathbf{S}_2\cdot\mathbf{S}_3) - 2J_{13}\mathbf{S}_1\cdot\mathbf{S}_3 \qquad (6)$$

$$\chi = \frac{-N}{H}\frac{\sum_i \frac{\delta E}{\delta H}\exp(-E_i/kT)}{\sum_i \exp(-E_i/kT)} \qquad (7)$$

combination with the thermodynamic expression for susceptibility (eq 7), directly yields the shape of the magnetic moment data at low temperatures. As discussed below, discrepancies between observed and calculated moments point to a small contribution from ZFS in some cases which becomes more evident at low temperatures and high fields. Zero-field terms are not included in eq 6. Use of Van Vleck's equation predicts a plateau in $\mu$ at low temperatures rather than a decrease. The possibility[55] that the physical effect of crystallite orientation and torquing at low temperatures and high fields contributes to the shape of the $\mu_{max}$ region can be eliminated since the data are reproducible whether the sample is a loose or pressed powder, and also, no magnetization is retained on raising and then lowering the field as has been observed with other systems.[56]

Our own calculations, and those made elsewhere by Kahn,[22] Chaudhuri,[24] Glerup,[57] and Drillon,[58] show that the irregular spin-state ladder can give rise to $\mu$/temperature plots of the type observed here. A convenient way to display the effect that the signs of $J_{12}$ and $J_{13}$ and the ratio $\alpha$ ($=J_{13}/J_{12}$) have on the energies of the zero-field $S$ spin levels is given in Figure 3. $\alpha$ is plotted against the energies for $J_{12}$ being either anti- or ferromagnetic in sign. Clearly, also, the spin of the ground state can change as $\alpha$ changes. A $S = 4$ ground state will occur, either when $J_{12}$ is negative (antiferromagnetic) and when $\alpha$ is less than +0.2 or when $J_{12}$ is positive and $\alpha$ is in the range $-0.25$ to $-0.33$. The reason for the rapid decrease in $\mu$ at very low temperatures is not immediately obvious from Figure 3a. It arises from thermal depopulation of the highest lying $M_S$ Zeeman levels of the ground $S = 4$ state, a feature also noted in a recent study by Kahn and Girerd *et al.*[59] in regard to a linear trinuclear $Mn^{II}$ carboxylate.

Wide ranges of parameter space were explored in order to try to fit the $\mu$/temperature data, with initial emphasis being given to fit the 4.2−70 K region and then the whole temperature range. A unique set of parameters was sought which yielded fits to the data measured in the various field strengths. It can be seen in Table 1 that the best fit to the whole temperature range for the various fields, obtained at each field by least-squares fitting, showed some variations but some commonality. $J_{12}$ is negative and in the range $-20 \pm 9$ cm$^{-1}$, the variations being probably due to fitting a wide temperature range and getting crossing of observed and calculated data, particularly at high temperatures in which, as described below, the shape of the curve does not follow the calculated broad minimum in $\mu$. $J_{13}$ is positive and in the range $4.5 \pm 2.5$ cm$^{-1}$. Use of negative values for $J_{13}$, a situation recently found[24] in a single-field study on an isoelectronic $Fe^{III}$−$Ni^{II}$−$Fe^{III}$ dimethylglyoximate-bridged trimer, gave notably worse fits. Calculations using Hamiltonian (6) show that, for $J_{12} = -20$ cm$^{-1}$, a gradual change in $J_{13}$ from +4 cm$^{-1}$ to −2.5 cm$^{-1}$ (i.e. $\alpha = -0.20$ to +0.125) results in (i) a decrease in $\mu$ (300 K) to 7.8 $\mu_B$, (ii) a steeper minimum in $\mu$ which occurs at lower $\mu$ and lower temperature as $\alpha$ becomes more positive, e.g. $\mu_{min} = 7.45$ $\mu_B$ at $T_{min} = 120$ K for $\alpha = +0.125$, and (iii) a much sharper $\mu_{max}$ shape with the $\mu_{max}$ and $T_{max}$ values decreasing as $J_{13}$ becomes more negative, e.g. 8.7 $\mu_B$ at $T_{max} = 8$ K for $\alpha = +0.125$. When $J_{13}$ is more negative than −4 cm$^{-1}$ (i.e. $\alpha > +0.2$) then the ground state changes successively to $S = 3$, 2, etc. and the low-temperature $\mu/T$ behavior is correspondingly quite different from that observed here. The $\alpha$ value here is $-0.22 \pm 0.02$ compared to +0.15 in the $Fe^{III}$−$Ni^{II}$−$Fe^{III}$ example, the latter having quite different bridging pathways. $g_{Fe}$ was assumed equal to $g_{Ru}$ and was allowed to vary for best fit, reaching a value of $2.0 \pm 0.04$. If $\alpha$ is kept constant, for instance in the 1 T data, and $J_{12}$ is set at a much larger value of −100 cm$^{-1}$, then there is a large discrepancy between observed and calculated data since the latter are those expected for an isolated $S = 4$ state. The size of $J_{12}$ is discussed further below.

**Table 1.** Best-Fit Parameters for (salmah)FeORu(TPP)OFe(salmah) over Temperature Range 300−4.2 K under Various Applied Fields

| field, $H$ (T) | $g_{Fe} = g_{Ru}$ | $J_{12}$ (cm$^{-1}$) | $J_{13}$ (cm$^{-1}$) | $\alpha = J_{13}/J_{12}$ |
|---|---|---|---|---|
| 0.1 | 2.02 | −15.3 | 2.1 | −0.14 |
| 0.3 | 1.96 | −29.1 | 7.2 | −0.25 |
| 1.0 | 1.95 | −19.7 | 6.5 | −0.33 |
| 3.0 | 2.04 | −11.3 | 2.1 | −0.19 |
| 3.0[a] | 1.95 | −32.7 | 8.2 | −0.25 |

[a] $g$ held at the 1.0 T best-fit value. The fit is better than that with $g = 2.04$ above 150 K but worse below 50 K, particularly in the region of the maximum in $\mu$.

The plot of $\mu$ at 4.2 K, versus applied field, is shown in Figure 4 and shows a reasonably good fit to the curve calculated using the best-fit parameters deduced, as described above for the 1 T field, *viz.* $g = 1.95$, $J_{12} = -19.7$ cm$^{-1}$, and $J_{13} = +6.3$ cm$^{-1}$. The deviations between observed and calculated values are probably due to the omission of zero-field splitting terms in the model. An alternative view of the field dependence at 4.2 K and at 10 K contains the magnetization isotherms given in Figure 5. The 10 K data fit very well for the $S = 4$ ground-state Brillouin function at all fields, while the 4.2 K data show deviations at high fields, again probably due to zero-field splitting of the $S = 4$ state.

The observed single-field data in the range 70−300 K show a gradual decrease in $\mu$ with increase in temperature and hint of a broad shoulder at *ca.* 150 K, compared to the broad minimum which is calculated. The same overall shape was observed for the two other $Fe^{III}Ru^{IV}Fe^{III}$ examples described in (b), below. Differences between observed and calculated data in this temperature region were, of course, worrying, and a number of reasons are possible for them. The possible effects of crystallite orientation have been discussed earlier and appear not to be occurring in the present system. Problems with temperature control and calibration in the Squid instrument can be eliminated, as discussed in the Experimental Section and by

(55) Wieghardt, K.; Chaudhuri, P.; Birkelbach, F. Personal communication, 1994.
(56) Kennedy, B. J.; Murray, K. S. *Inorg. Chem.* **1985**, *24*, 1552.
(57) Corbin, K. M.; Glerup, J.; Hodgson, D. J.; Lynn, M. H.; Michelsen, K.; Nielsen, K. M. *Inorg. Chem.* **1993**, *32*, 18.
(58) Drillon, M.; Darriet, J. *Struct. Bonding* **1992**, *79*, 55.
(59) Menage, S.; Vitols, S. E.; Bergerat, P.; Codjovi, E.; Kahn, O.; Girerd, J.-J.; Guillot, M.; Solans, X.; Calvet, T. *Inorg. Chem.* **1991**, *30*, 2666.
(60) Mochizuki, K.; Kesting, F.; Weyermüller, T.; Wieghardt, K.; Butzlaff, C.; Trautwein, A. X. *J. Chem. Soc., Chem. Commun.* **1994**, 909.

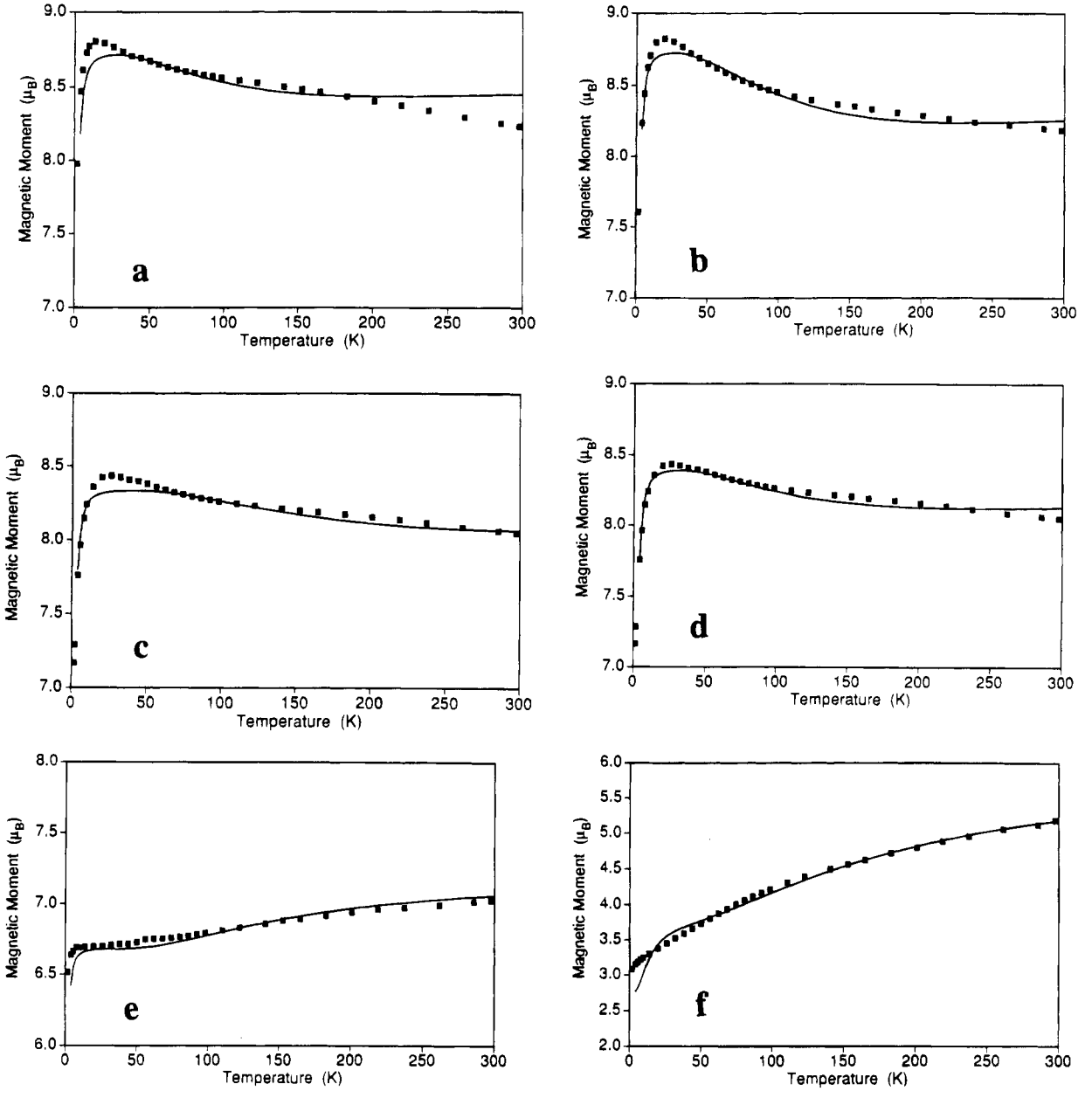


**Figure 2.** Plot of $\mu$ (per mol) versus temperature in an applied-field of 1 T for (a) (salmah)FeORu(TPP)OFe(salmah), where the solid line is that calculated using a $S = {}^5/_2{:}1{:}{}^5/_2$ model with the parameters given in Table 1, and (b) (TMP)FeORu(TPP)OFe(TMP), where the solid line is that calculated using a $S = {}^5/_2{:}1{:}{}^5/_2$ model with $g = 1.95$, $J_{12} = -23.4$ cm$^{-1}$, $J_{13} = +5.4$ cm$^{-1}$, and $\alpha = -0.23$, (c) (TPP)FeORu(TPP)OFe(TPP), where the solid line is that calculated using a $S = {}^5/_2{:}1{:}{}^5/_2$ model with $g = 2.0$, $J_{12} = -35.7$ cm$^{-1}$, $J_{13} = +11.2$ cm$^{-1}$, $\alpha = -0.31$, and % Fe(TPP)$_2$O (with $J = -100$ cm$^{-1}$) = 13, (d) (TPP)FeORu(TPP)OFe(TPP), where the solid line is that calculated using a $S = {}^5/_2{:}1{:}{}^5/_2$ model with $g = 1.88$, $J_{12} = -22.2$ cm$^{-1}$, $J_{13} = +7.8$ cm$^{-1}$, and $\alpha = -0.35$, (e) (TMP)MnORu(TPP)OMn(TMP), where the solid line is that calculated using a $S = 2{:}1{:}2$ model with $g = 1.93$, $J_{12} = -17.4$ cm$^{-1}$, $J_{13} = +9.6$ cm$^{-1}$, and $\alpha = 0.55$, and (f) (TPP)CrORu(TPP)OCr(TPP), where the solid line is that calculated using a $S = {}^3/_2{:}1{:}{}^3/_2$ model with $g = 1.98$, $J_{12} = -25.3$ cm$^{-1}$, $J_{13} = -11.1$ cm$^{-1}$, and $\alpha = 0.44$.

relation to many contemporaneous measurements on unrelated samples. Indeed, the first measurements on the present compounds were made on a well-calibrated Faraday balance and the same shaped $\mu/T$ plots were obtained. It seems most likely that, despite the care exercized in sample isolation and purification, the reason for the differences is chemical in origin, perhaps a minor component of a second species being present but one not discernible by Mössbauer measurements. Syntheses and purification of the present trinuclear metalloporphyrin species are demanding, not trivial, and are complicated by solvation effects in crystalline samples. Furthermore, it is possible that the lack of an observed minimum in $\mu$ in the 70−300 K region is, in part, due to effects such as spin−orbit coupling on Ru[IV] (ref 60) and/or the effect of population of nearby excited states neither of which are included in the model.

The spin ladder appropriate to the parameters obtained at 1 T is shown in Figure 6. The energy gap between the |4,5> ground state and the next higher state (|3,4>), of 104 cm$^{-1}$, means that the decrease in $\mu$ at very low temperatures is due to thermal depopulation of $M_S$ levels from the ground state. For comparison, we note that a separation of only 15 cm$^{-1}$ was appropriate to the best-fit values obtained for the Fe[III]−Ni[II]−Fe[III] dimethylglyoximate complex of Chaudhuri *et al.* ($J_{12} = -32$ cm$^{-1}$, $J_{13} = -5$ cm$^{-1}$).[24]

There are two interesting and, perhaps, unexpected features of the magnetism of this Fe[III]−O−Ru[IV]−O−Fe[III] system which deserve further comment. First, the $J_{12}$ value is smaller in size than might be anticipated from the large negative values obtained in Fe[III]−O−Fe[III] and Ru[IV]−O−Ru[IV] complexes, the latter probably being better represented by a molecular orbital

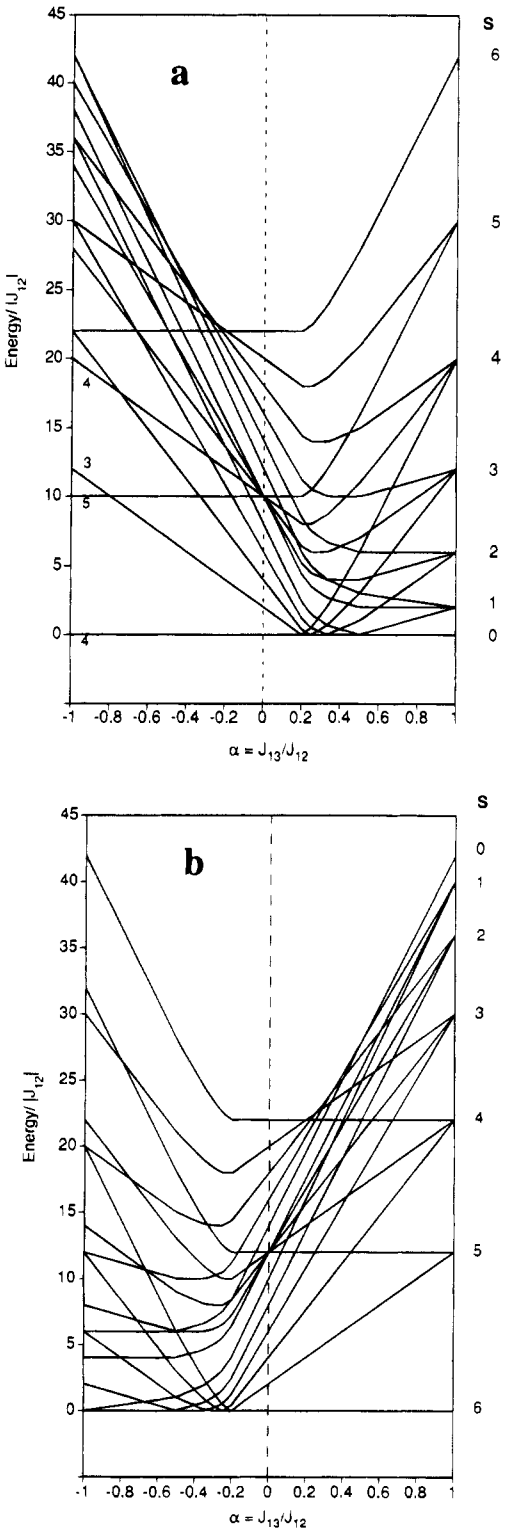


**Figure 3.** Calculated zero-field energy levels (energy/$|J_{12}|$) as a function of α for a $S = {}^5/_2{:}1{:}{}^5/_2$ model with (a) $J_{12}$ negative and (b) $J_{12}$ positive.

description,[61,62] with spin-pairing in the HOMO levels, than by a Heisenberg spin coupling model of the type used here and for the $Fe^{III}-O-Fe^{III}$ species.[63,64] A recent example of a μ-oxo $Ru^{IV}\cdots Fe^{III}$ dinuclear complex, containing also two μ-carboxylate bridges *viz.* $[(Me\text{-}tacn)Ru^{IV}(\mu\text{-}O)(\mu\text{-}CH_3CO_2)_2Fe^{III}(tacn)]^{3+}$

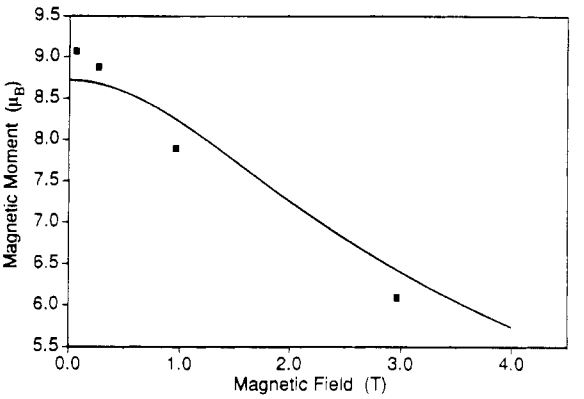


**Figure 4.** Plot of μ (per mol) versus applied field for (salmah)FeORu(TPP)OFe(salmah), measured at 4.2 K. The solid line is that calculated using the $S = {}^5/_2{:}1{:}{}^5/_2$ model with the parameter set given in Table 1 for the 1 T field.

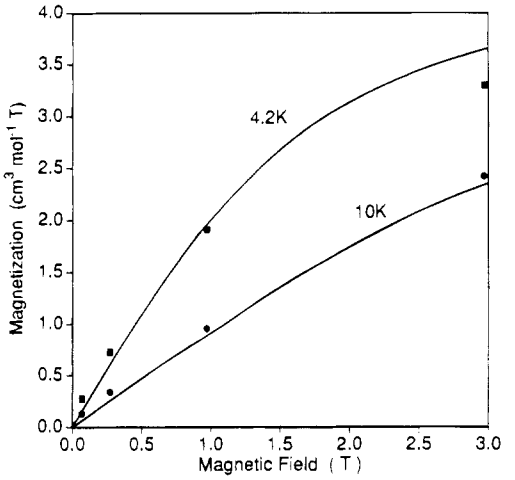


**Figure 5.** Plots of magnetization (per mol) versus applied field for (salmah)FeORu(TPP)OFe(salmah) at 4.2 and 10 K. The solid lines are the Brillouin functions for a spin = 4 state with $g = 1.95$.

showed very strong antiferromagnetic coupling leading to a $S = {}^3/_2$ ground state at all temperatures.[21] Interestingly, while these tribridged species obviously have different bridging geometries (Ru−O−Fe = 121°) compared to the singly-bridged μ-oxo−porphyrin compounds, the related dinuclear complexes $(P)Cr^{III}(\mu\text{-}O)Fe^{III}(P)$[11a] showed similar sized $J$ values to their $[tacnCr^{III}(\mu\text{-}O)(\mu\text{-}RCO_2)_2Fe^{III}tacn]^{2+}$ counterparts.[65] In $\mu_3$-oxo-bridged tri- or tetranuclear complexes it is well-known that $J$ values appropriate to a M−O−M′ bridge are significantly less than those in $\mu_2$-oxo-bridged dinuclear analogues, even after allowing for different M−O−M angles and M···M distances, and this no doubt relates to competing exchange pathways in the $\mu_3$-oxo-bridged systems some of which can be ferromagnetic in nature thus leading to lower net $J$ values.[1,66] This may play a part in the present type of linear trimer in which, while the $\mu_2$-oxo bridges do not experience competing pathways, the central $Ru^{IV}$ "bridge" does have to share itself two ways with the Fe salmah units which are eclipsed in relation to each other. Related differences in $J_{MM'}$ values between some other M−X−M′−X−M and M−X−M′ systems have been noted previously.[23,26,27,57,67] Geometric differences noted in (salmah)Fe(μ-O)Ru(TPP)(μ-O)Fe(salmah) compared to $Fe^{III}OFe^{III}$ and

(61) Dunitz, J. D.; Orgel, L. E. *J. Chem. Soc.* **1953**, 2594.
(62) Gafford, B. G.; Marsh, R. E.; Schaefer, W. P.; Zhang, J. H.; O'Connor, C. J.; Holwerda, R. A. *Inorg. Chem.* **1990**, *29*, 4652.
(63) Murray, K. S. *Coord. Chem. Rev.* **1974**, *12*, 1.
(64) Kurtz, D. M., Jr. *Chem. Rev.* **1990**, *90*, 585.
(65) Hotzelmann, R.; Wieghardt, K.; Flörke, U.; Haupt, H. J.; Weatherburn, D. C.; Bonvoisin, J.; Blondin, G.; Girerd, J.-J. *J. Am. Chem. Soc.* **1992**, *114*, 1681.
(66) Blake, A. B.; Yavari, A.; Hatfield, W. E.; Sethulekshmi, C. N. *J. Chem. Soc., Dalton Trans.* **1985**, 2509.
(67) Kahn, O. *Struct. Bonding* **1987**, *68*, 89.

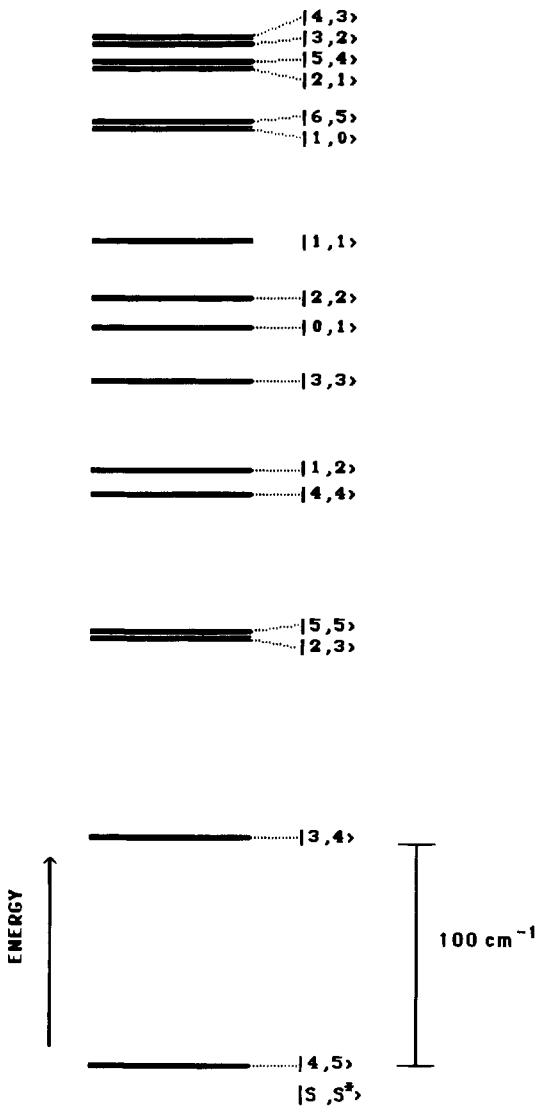


**Figure 6.** Zero-field energy levels ("spin ladder") for (salmah)FeORu(TPP)OFe(salmah) appropriate to the best-fit parameters given in Table 1.

Ru$^{IV}$ORu$^{IV}$ analogues, such as the Fe−O−Ru angle (155.2(5)°) compared to RuORu angles of *ca.* 180°, the Fe−O bond length of 1.848(6) Å compared to those of *ca.* 1.75−1.82 Å in most FeOFe complexes,[63,64] and the Ru−O length 1.866(6) Å compared to 1.820(8) Å in the Ru$^{IV}$O(OAc)$_2$Fe$^{III}$ tacn complex,[21] may also play a part in the resultant size of $J_{12}$. It should be noted that the $J_{12}$ values deduced for the Cr$^{III}$−O−Ru$^{IV}$−O−Cr$^{III}$ and Mn$^{III}$−O−Ru$^{IV}$−O−Mn$^{III}$ analogues, described below, are also much lower than would be anticipated from typical Cr$^{III}$−O−Cr$^{III}$ and Mn$^{III}$−O−Mn$^{III}$ $J$ values.[68,69]

From the Goodenough−Kanamori superexchange picture of orbital overlap in the present system,[1] the $\mu$-oxo atom in each half forms a corner which is shared by two octahedrally coordinated Fe$^{III}$ and Ru$^{IV}$ ions. The M−($\mu$-O) $z$-directions are not precisely collinear because of the bent FeORu angle. Nevertheless, the dominant interaction will be between Ru$^{IV}$-($d_{xz}$, $d_{yz}$)$^2$, Fe$^{III}$($d_{xz}$, $d_{yz}$)$^2$, and the $p_x$, $p_y$ orbitals of the bridging oxygen, which provides an antiferromagnetic $\pi$-pathway. Potential antiferromagnetic $\sigma$-pathways involving metal $d_{z^2}$ and oxygen $p_z$ orbitals are attenuated because of the empty Ru$^{IV}$ orbital. The recent model of Wieghardt and Girerd *et al.*[65] gives a similar picture except that the largest overlap of magnetic orbitals in the Ru$^{IV}$($\mu$-O)($\mu$-CH$_3$CO$_2$)$_2$Fe$^{III}$ system are calculated to be $d_{yz}$, $d_{yz}$ and the "crossed" interaction $d_{z^2}$, $d_{xz}$, the former leading to antiferromagnetic $J^{AF}_{yz,yz}$ and the latter to ferromagnetic $J^{F}_{z^2,xz}$, since the Ru$^{IV}$ $d_{z^2}$ orbital is empty.[21] The $J^{F}_{z^2,xz}$ contribution to $J_{12}$ was deemed to be very weak in the dinuclear example on account of energy mismatch of $4d_{z^2}$ and $3d_{xz}$ orbitals. One might anticipate a similar conclusion here. We have shown, recently, that the present kind of geometry in dinuclear $\mu$-oxo Fe$^{III}$ (low-spin) phthalocyanines, which involve $t_{2g}^5$ orbitals on both Fe$^{III}$ atoms, does lead to net ferromagnetism.[70] Thus, in view of these various arguments, it may not be surprising that $J_{12}$ is overall weakly antiferromagnetic in the present M$^{III}$−O−Ru$^{IV}$ fragments.

The second point of interest is the ferromagnetic sign of $J_{13}$ found between the terminal Fe$^{III}$ atoms, the coupling apparently occurring over a large distance of *ca.* 7.2 Å and which must, presumably, involve the central Ru(TPP) moiety. The opposite sign of $J_{13}$ was found for Chaudhuri's dimethylglyoximato-bridged Fe$^{III}$Ni$^{II}$Fe$^{III}$ complex which had a similar Fe$^{III}$···Fe$^{III}$ separation, and this was rationalized in terms of interactions solely via the delocalized dmg$^{2-}$ ligand pathways.[24] We do not have a ready explanation for the sign of $J_{13}$, particularly since it is negative in the Cr$^{III}$ case (but see arguments, below). However, we note that there are a number of linear trinuclear systems in which $J_{13}$ has recently been found to be positive and these often involve thiolates or chalcogenido bridges, albeit with terminal M···M separations rather smaller than that given here.[27,55] Indeed, one such case had a diamagnetic central metal, Co$^{III}$. In these and the present system, it is possible to write spin-polarization schemes which lead to parallel spin coupling on the terminal ions, but further work is required in order to sort out this phenomenon. It is interesting to note that weak spin exchange has recently been postulated to explain the ESR signal in some heterotrinuclear Ru$^{II}$TPP complexes which contain two *trans*-axial $\mu$-4,4′-bipyridine−Mo(NO)(Cl)(HB(Me$_2$pz)$_3$) spin = $^1/_2$ centers, spaced some 16 Å apart.[71]

**(b) (TPP)FeORu(TPP)OFe(TPP) and (TMP)FeORu(TPP)OFe(TMP).** The $\mu$/temperature plots at 1 T for these complexes were similar in shape to that described above for the Fe(salmah) example. The Fe(TMP) complex yielded a reasonably good fit particularly at the low temperature end, as shown in Figure 2b for the following set of parameters:

$$g = 1.95 \quad J_{12} = -23.4\ \text{cm}^{-1}$$
$$J_{13} = +5.4\ \text{cm}^{-1} \quad \alpha = -0.23$$

The Fe(TPP) complex showed lower $\mu$ values than the other two with $\mu_{max}$, in particular, being only 8.4 $\mu_B$, even lower than the $S = 4$ calculated value. There are a number of possible reasons for such a low $\mu_{max}$ value. First the "nonsolvated" molecular weight employed may have been less than it should be because of solvation effects. However, microanalytical data, while not always unambiguous in such high molecular weight species, would preclude this and, also, the data were reproducible from sample to sample. Second, it may contain some fraction of strongly coupled [Fe(TPP)]$_2$O which is a common byproduct in this chemistry (*vide infra*) and which is diamagnetic in the $\mu_{max}$ region.[63,64] Such an impurity would not be detected in the Mössbauer spectrum, which, while displaying an asym-

(68) Hodgson, D. J. *Prog. Inorg. Chem.* **1975**, *19*, 173.
(69) Wieghardt, K. *Angew. Chem., Int. Ed. Engl.* **1989**, *28*, 1153.
(70) Sievertsen, S.; Murray, K. S.; Moubaraki, B.; Berry, K. J.; Korbatieh, Y.; Cashion, J. D.; Brown, L. J.; Homborg, H. *Z. Anorg. Chem.* **1994**, *620*, 1203.
(71) McCleverty, J. A.; Navar Badida, J. A.; Ward, M. D. *J. Chem. Soc., Dalton Trans.* **1994**, 2415.

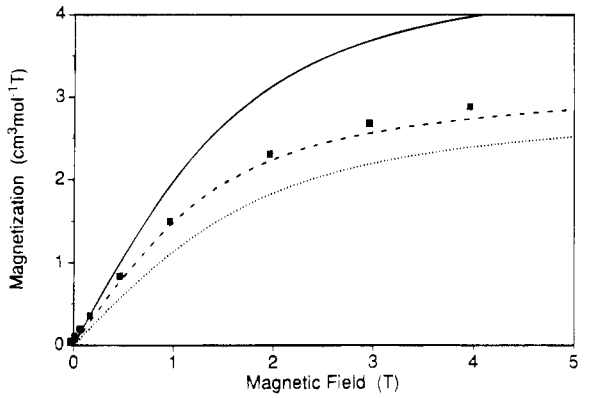


**Figure 7.** Plot of magnetization (per mol) (■) for (TPP)FeORu(TPP)-OFe(TPP) at 4.2 K. The lines are shown are those calculated using $g = 2.0$ for (a) a Brillouin function for spin = 4 (—), (b) a zero-field split spin = 4 state with $D = 5$ cm$^{-1}$ (- - -), and (c) a zero-field split spin = 4 state with $D = 10$ cm$^{-1}$ (•••).

metric doublet, yields the same $\delta$ and $\Delta E_Q$ values as does [Fe(TPP)]$_2$O.[63,64] Indeed, if a 13% "impurity" of the $\mu$-oxo Fe$^{III}$ species is assumed (with $J = -100$ cm$^{-1}$), a reasonably good fit to the data can be achieved for parameter values $g = 2.0$, $J_{12} = -35.7$ cm$^{-1}$, $J_{13} = 11.2$ cm$^{-1}$, and $\alpha = -0.31$. The $\mu_{max}$ and $\mu$(< 8 K) regions show some divergences from theory (Figure 2c). Third, the data may reflect a $g$ value lower than 2.0 as postulated recently for a heterotetranuclear $\mu$-oxo Cr$^{III}$•••Mn$^{III}$ system (*viz.* $g = 1.71$).[72] It is possible to get a reasonable fit using the parameter set $g = 1.88$, $J_{12} = -22.2$ cm$^{-1}$, $J_{13} = 7.8$ cm$^{-1}$, and $\alpha = -0.35$ (Figure 2d), although the agreement in the graph above 100 K and below 10 K is not good. Discrepancies at very low temperatures were also evident in the magnetization isotherms made on this complex at 4.2 K in fields of 0.3, 0.5, 1.0, 2.0, 3.0, and 4.0 T. A Brillouin calculation for $S = 4$, with $g = 1.88$, overestimated the observed magnetization and $\mu$ values, particularly at large fields. This strongly suggests that zero-field splitting of the $S = 4$ state, originating from Fe$^{III}$TPP, or spin−orbit coupling of the Ru$^{IV}$ center,[60] needs to be considered in this case since it is more evident than in the other FeORuOFe compounds discussed. Inclusion of zero-field splitting of the $S = 4$ state using $D = 5$ cm$^{-1}$ and $g = 2.0$ did, indeed, give much better agreement with the magnetization data (Figure 7).

**(c) (TMP)MnORu(TPP)OMn(TMP).** As indicated above, apart from the (TMP)MnORu(TMP)OMn(TMP) complex, which has a lower moment than the others, these spin = 2:1:2 compounds all have $\mu$ values of 7.0 ± 0.2 $\mu_B$ at 295 K. The title compound shows a gradual decrease in $\mu$ as the temperature is decreased, until a plateau value of 6.7 $\mu_B$ is obtained below *ca.* 70 K. A rapid decrease in $\mu$ occurs below 10 K with a value of 6.5 $\mu_B$ being attained at 4.2 K (Figure 2e). The combination of the 295 K $\mu$ value and the plateau value are symptomatic of a weakly coupled system with a <3,4| ground state, although the plateau value is a little lower than that anticipated for $S = 3$, *viz.* 6.93 $\mu_B$. This is reflected in the $g$ value of 1.93 being obtained for best fit. Use of the appropriate trimer model yielded $g = 1.93$, $J_{12} = -17.4$ cm$^{-1}$, $J_{13} = +9.6$ cm$^{-1}$, and, hence, $\alpha = J_{13}/J_{12} = -0.55$. Calculations of the energy levels show that, for $J_{12}$ negative, $S = 3$ becomes the ground state when $\alpha$ is less than 0.25. Exploration of various values of $J_{12}$ and $J_{13}$, for a $S = 3$ ground level situation, shows that the precise shape of the $\mu$/temperature plot at temperatures above the plateau region, including whether or not a dip in $\mu$ is shown, depends sensitively on the size of $J_{12}$ and the ratio $\alpha$ of $J_{13}/J_{12}$. The rapid decrease in $\mu$ at very low temperatures is due, again, to thermal depopulation of the $M_S = 3$ Zeeman sublevels.

The values and signs of $J_{12}$ and $J_{13}$ are broadly similar to those found for the FeRuFe compounds described above. There is precedence for one other spin 2:1:2 combination available in the case of Chaudhuri's complex, [(Me-tacn)Mn{$\mu$-(dmg)$_3$Ni}-Mn(Me-tacn)]$^{2+}$, for which somewhat similar parameters were found, although the positive sign of $J_{13}$ is presently under doubt.[73] The size of $J_{12}$ in the present complex is lower than might be expected in relation to Mn$^{III}$−O−Mn$^{III}$ systems[69] and, again, presumably is related to the unfavorable overlap of Mn, $\mu$-oxo, and Ru orbitals as described above for the Fe$^{III}$ system.

**(d) (TPP)CrORu(TPP)OCr(TPP).** The moment of this complex decreases gradually from 5.2 $\mu_B$ at 295 K to 3.0 $\mu_B$ at 4.2 K without any evidence of a low temperature plateau (Figure 2f). Calculations for this spin $^3/_2$:1:$^3/_2$ system show that, when $J_{12}$ is negative, the possible ground states and their ranges of $\alpha$ are as follows:

$$S = 2 \qquad \alpha \leq {}^1/_3$$

$$S = 1 \qquad {}^1/_3 \leq \alpha < {}^1/_2$$

$$S = 0 \qquad \alpha \geq {}^1/_2$$

Since the observed $\mu$ is much less than 4.9 $\mu_B$ at 4.2 K, the coupled ground state must be either $S = 1$ or 0, and the latter can be discounted since $\mu$ is much higher than zero. A reasonable fit to the data, shown in Figure 2f, was obtained for the parameter set appropriate to a $S = 1$ ground state: $g = 1.98$, $J_{12} = -25.3$ cm$^{-1}$, $J_{13} = -11.1$ cm$^{-1}$, and $\alpha = 0.44$. The main deviations occur below 50 K. Magnetization data obtained using fields of 0.1−5.0 T, at temperatures between 3.5 to 8 K, confirmed the $S = 1$ ground state and gave, upon fitting to eq 6, more realistic parameter values, *viz.* $J_{12} = -25 \pm 1$ cm$^{-1}$, $J_{13} = -10 \pm 1$ cm$^{-1}$, and $\alpha = +0.4 \pm 0.1$.

A recent "open-form" trinuclear $\mu$-hydroxo complex, [(H$_2$O)(pico)Cr($\mu$-OH)Ni(H$_2$O)$_4$($\mu$-OH)Cr(pico)(OH)]$^{4+}$, where pico is (2-pyridyl)methylamine, described by Glerup *et al.*[57] and having a $^3/_2$:1:$^3/_2$ spin combination also showed $J_{12}$ and $J_{13}$ to be negative (−4.2 and −1.5 cm$^{-1}$, respectively). The $\alpha$ value of 0.34 was assigned to a $S = 2$ ground state. The antiferromagnetic Cr••Ni coupling was ascribed, by use of the model of Glerup *et al.*,[74] to a balance between $\pi-\pi$ (ferromagnetic) and $\pi-\sigma$ (antiferromagnetic) interactions. Related arguments can be put forward in the present fragment, *viz.* {Cr$^{III}$(half-filled $\pi$, empty $\sigma$)−Ru$^{IV}$(partly filled $\pi$, empty $\sigma$)}. Both studies agree on a negative Cr••Cr exchange interaction, spanning some 8 Å in the Cr($\mu$-OH)Ni($\mu$-OH)Cr spine and some 7.4 Å (assumed) in the present Cr($\mu$-O)Ru($\mu$-O)Cr spine. The presence of hydrogen in the $\mu$-OH bridge probably leads to the smaller size of $J_{12}$ in the $\mu$-hydroxo compared to the $\mu$-oxo compound.

## Conclusions

A redox reaction involving Ru$^{VI}$(O)$_2$(porphyrin) and a M$^{II}$(L) Schiff base or porphyrin complex has been successfully used to prepare a series of trinuclear $\mu$-oxo complexes of type (L)M$^{III}$ORu$^{IV}$(P)OM$^{III}$(L), where M = Fe, Cr, and Mn. The crystal structure has been solved for one of the Fe$^{III}$ORu$^{IV}$OFe$^{III}$

(72) Chaudhuri, P.; Birkelbach, F.; Winter, M.; Staemmler, V.; Fleischauer, P.; Haase, W.; Flörke, U.; Haupt, H.-J. *J. Chem. Soc., Dalton Trans.* **1994**, 2313.

(73) Chaudhuri, P. Personal communication, 1994.

(74) Glerup, J.; Hodgson, D. J.; Pedersen, E. *Acta Chem. Scand.* **1983**, *A37*, 161.

examples confirming the linear array of metal ions and bent FeORu bridges.

A combination of variable temperature and variable field magnetic susceptibility measurements has been used to deduce the ground state, the spin ladder of energy levels, and the exchange parameters $J_{12}$ and $J_{13}$ in these exchange-coupled systems. The $J_{13}$ parameter cannot be set to zero as is commonly done. The importance has been emphasized of $\alpha$, the ratio of $J_{13}/J_{12}$, in determining the energies of the coupled spin states which arise in these mixed-spin systems. The importance of using the thermodynamic, field-dependent form of the susceptibility equation for conditions of low temperature and high field values, rather than the Van Vleck equation, was also stressed.

The $J_{12}$ values are generally much smaller in size than those observed previously for the analogous binuclear $Ru^{IV}ORu^{IV}$ and $M^{III}OM^{III}$ species. Possible reasons for these differences have been given. Possible reasons for the size and sign of $J_{13}$ values have also been presented.

**Acknowledgment.** This work was supported by grants from the Australian Research Council (to B.O.W. and K.S.M.), an Australian Postgraduate Research Award (to L.D.S.), and an Australian Research Council Postdoctoral Fellowship (to B.M.). The help of Dr. A. Markiewicz with preliminary magnetic measurements and of Associate Professor J. D. Cashion and Mr. Y. Korbatieh with Mössbauer spectral measurements is gratefully acknowledged.

**Supporting Information Available:** Table S1, containing microanalytical and infrared data for the trinuclear complexes (1 page). Ordering information is given on any current masthead page.

IC9414435